Clinical Research in Cardiology (2020) 109:735–745
https://doi.org/10.1007/s00392-019-01562-3

ORIGINAL PAPER

Correlation of machine learning computed tomography-based fractional flow reserve with instantaneous wave free ratio to detect hemodynamically significant coronary stenosis

Stefan Baumann[1,2,11] · Markus Hirt[1,2] · U. Joseph Schoepf[3] · Marlon Rutsch[1,2] · Christian Tesche[4] · Matthias Renker[5] · Joseph W. Golden[3] · Sebastian J. Buss[6] · Tobias Becher[1,2,7] · Waldemar Bojara[8] · Christel Weiss[9] · Theano Papavassiliu[1,2] · Ibrahim Akin[1,2] · Martin Borggrefe[1,2] · Stefan O. Schoenberg[10] · Holger Haubenreisser[10] · Daniel Overhoff[10] · Dirk Lossnitzer[1,2]

Received: 11 July 2019 / Accepted: 17 October 2019 / Published online: 29 October 2019

Abstract

Background Fractional flow reserve based on coronary CT angiography (CT-FFR) is gaining importance for non-invasive hemodynamic assessment of coronary artery disease (CAD). We evaluated the on-site CT-FFR with a machine learning algorithm ($CT\text{-}FFR_{ML}$) for the detection of hemodynamically significant coronary artery stenosis in comparison to the invasive reference standard of instantaneous wave free ratio (iFR®).

Methods This study evaluated patients with CAD who had a clinically indicated coronary computed tomography angiography (cCTA) and underwent invasive coronary angiography (ICA) with iFR®-measurements. Standard cCTA studies were acquired with third-generation dual-source computed tomography and analyzed with on-site prototype $CT\text{-}FFR_{ML}$ software.

Results We enrolled 40 patients (73% males, mean age 67 ± 12 years) who had iFR®-measurement and $CT\text{-}FFR_{ML}$ calculation. The mean calculation time of $CT\text{-}FFR_{ML}$ values was 11 ± 2 min. The $CT\text{-}FFR_{ML}$ algorithm showed, on per-patient and per-lesion level, respectively, a sensitivity of 92% (95% CI 64–99%) and 87% (95% CI 59–98%), a specificity of 96% (95% CI 81–99%) and 95% (95% CI 84–99%), a positive predictive value of 92% (95% CI 64–99%), and 87% (95% CI 59–98%), and a negative predictive value of 96% (95% CI 81–99%) and 95% (95% CI 84–99%). The area under the receiver operating characteristic curve for $CT\text{-}FFR_{ML}$ on per-lesion level was 0.97 (95% CI 0.91–1.00). Per lesion, the Pearson's correlation between the $CT\text{-}FFR_{ML}$ and iFR® showed a strong correlation of $r = 0.82$ ($p < 0.0001$; 95% CI 0.715–0.920).

Conclusion On-site $CT\text{-}FFR_{ML}$ correlated well with the invasive reference standard of iFR® and allowed for the non-invasive detection of hemodynamically significant coronary stenosis.

Keywords Coronary artery disease · Coronary CT angiography · Fractional flow reserve derived from coronary computed tomography angiography · Instantaneous wave-free ratio · Invasive coronary angiography · Myocardial ischemia

Abbreviations

CAD	Coronary artery disease
cCTA	Coronary computed tomography angiography
CT	Computed tomography
CT-FFR	Fractional flow reserve derived from coronary computed tomography angiography
$CT\text{-}FFR_{ML}$	Fractional flow reserve derived from coronary computed tomography angiography based on machine learning algorithm
ESC	European Society of Cardiology
FFR	Fractional flow reserve
ICA	Invasive coronary angiography
iFR®	Instantaneous wave free ratio

Introduction

Due to its high sensitivity and negative predictive value, coronary computed tomography angiography (cCTA) has become an established and helpful clinical tool to rule out

✉ Stefan Baumann
stefan.baumann@umm.de

Extended author information available on the last page of the article

obstructive coronary artery disease (CAD) in patients with low to intermediate pre-test probability [1, 2]. Yet, similar to invasive coronary angiography (ICA), cCTA provides only morphological assessment. In clinical practice an increasing number of unnecessary ICAs in cases of non-obstructive CAD are performed [3, 4] due to the tendency of cCTA to overestimate the severity of stenosis, as expected given the comparatively moderate specificity of cCTA [5]. Furthermore, two previous studies, the prospective multicenter imaging study for evaluation of chest pain (PROMISE) and SCOT-HEART, were inconsistent in their conclusions on the role of cCTA in the disease management plan of patients with CAD [6, 7].

It is now possible to calculate resting flow dynamics by cCTA-based fractional flow reserve (CT-FFR) [8]. With this technique, cCTA datasets can be assessed not only anatomically but also regarding the hemodynamic significance of lesions, which can be determined with no additional radiation exposure [9]. CT-FFR demonstrates strong correlation with invasive fractional flow reserve (FFR) [10, 11] and is gaining importance for non-invasive hemodynamic assessment of obstructive CAD [12–16]. Several large trials and meta-analyses demonstrate significant improvements in diagnostic accuracy compared to cCTA alone [17–22]. Moreover, the Food and Drug Administration approved the use of an off-site CT-FFR approach in 2015. An evolution in the development of CT-FFR is the development of an on-site prototype with a machine-learning algorithm (CT-FFR_{ML}). There has been a remarkable reduction of required computation time compared to CT-FFR based on computational fluid dynamics [23, 24].

FFR during invasive coronary angiography (ICA) is an established reference standard in the determination of the hemodynamic significance of coronary stenosis [25, 26]. However, in clinical practice, FFR measurements are limited by a variety of factors. E.g., the intravascular administration of adenosine involved in this procedure leads to numerous side effects, such as discomfort, dyspnea, and angina pectoris and often prolongs the ICA procedure [9, 27–29]. Instantaneous wave free ratio (iFR®) is an innovative approach and has generated interest for the invasive detection of hemodynamically significant coronary stenosis. With the use of pressure wires, iFR® isolates a specific period of time during diastole known as the wave-free period when microvascular resistance is low and stable and can then detect relevant coronary stenosis based on results of pressure and flow. iFR® was proven to be non-inferior to FFR but does not involve the need for hyperemia [30–32]. Therefore, iFR®, as a resting index, offers several substantial advantages, including the reduction of side effects and improvements of patient comfort by obviating the need of adenosine [30, 31, 33]. Accordingly, both FFR and iFR® have a class IA recommendation for determining the indication of revascularization in the European Society of Cardiology (ESC) guidelines of 2018 [34]. We aimed to investigate on-site CT-FFR_{ML} in terms of clinical practicability and diagnostic accuracy when compared to iFR® as one the current invasive reference standards to detect hemodynamically significant coronary artery stenosis.

Materials and methods

Patient population, study design

The local Institutional Review Board approved the study protocol (No. 2015-583N-MA). Written informed consent was obtained from all patients. Our prospective, single-center, and non-randomized study was applied to actual clinical settings, under the consideration of the current ESC-guidelines on myocardial revascularization [34]. The initial population of our study consisted of 80 patients with suspected CAD who underwent a clinically indicated cCTA between July 2017 and December 2018. General clinical exclusion criteria for performing cCTA were known contrast agent allergies, severely reduced left ventricular function, renal insufficiency, significant increase of high-sensitivity-troponin I (> 0.2 ng/mL), EKG signs of acute myocardial injury, and significant valvular pathology.

Specific exclusion criteria for on-site CT-FFR_{ML} calculation were severe left main disease, severe stenosis of the coronary ostium, serial lesions, complex bifurcation stenosis type D (SYNTAX score classification), aneurysms, severe diffuse disease, chronic total occlusion, previous percutaneous coronary stent implantation, previous coronary artery bypass grafting (CABG), or inadequate image quality of the cCTA dataset. Baseline characteristics and cardiovascular risk factors were obtained from medical records. In accordance with the recommendation of the ESC, the CAD consortium clinical score was applied to determine the pretest probability for CAD [35]. In addition, the impairment of left ventricular function was determined by echocardiography before cCTA. Acquisition of cCTA datasets was performed with a standard cCTA protocol. If cCTA showed a stenosis with the potential of hemodynamic relevance or uncertain finding, which was verified by a senior radiologist, an ICA was indicated. During ICA, the coronary arteries were evaluated by a senior interventional cardiologist. Visually intermediate grade stenotic lesions (40–80%) were evaluated by iFR®-measurement intraprocedurally for hemodynamic significance. In case the iFR® value was hemodynamically significant (≤ 0.89), revascularization was performed by percutaneous coronary intervention (PCI) or coronary artery bypass graft (CABG) [25, 26, 34]. After successful completion of cCTA and iFR®-measurements, the cCTA datasets were evaluated by on-site CT-FFR_{ML} (Fig. 1).

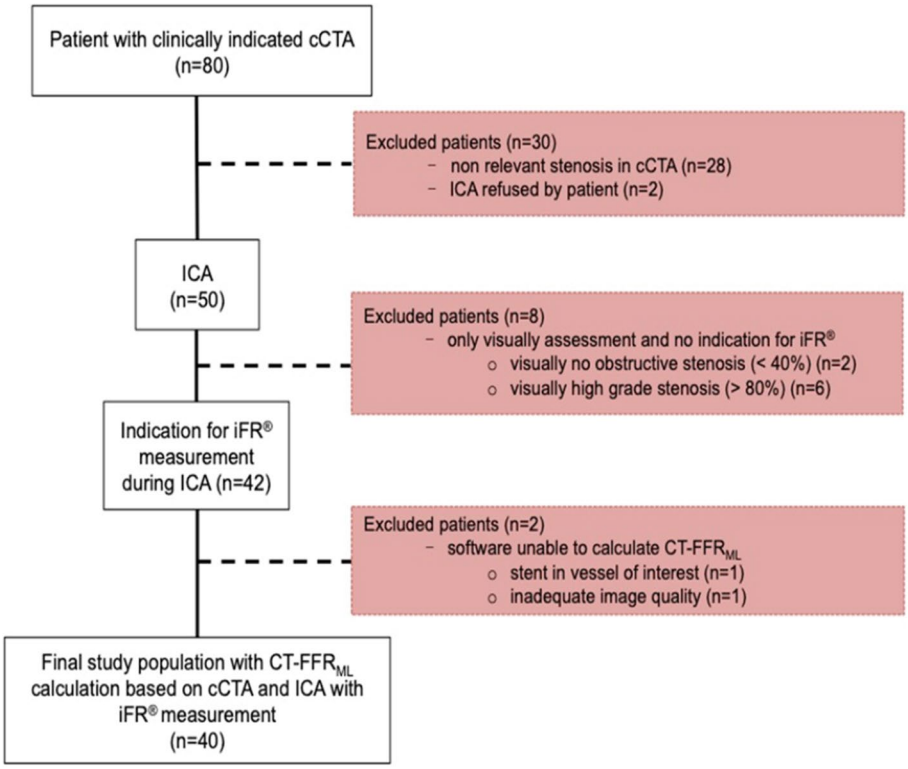

Fig. 1 Flowchart illustrates the enrollment process. *cCTA* coronary computed tomography angiography, *CT-FFR$_{ML}$* fractional flow reserve derived from coronary computed tomography angiography based on machine learning algorithm, *ESC* European Society of Cardiology, *ICA* invasive coronary angiography, *iFR®* instantaneous wave free ratio

Acquisition and analysis of cCTA datasets

Acquisition and analysis of cCTA data were performed according to the standard of care. After a non-contrast calcium scoring acquisition, cCTA was accomplished utilizing a low-dose protocol on a third-generation dual-source CT system (Siemens, Somatom FORCE, Siemens Healthineers). Sublingual nitroglycerin was administered prior to cCTA and beta-blockers were given to achieve a resting heart rate below 65/min. An injection of 80 mL of iodinated contrast material (Iomeron 400; Bracco Imaging S.p.A., Milan, Italy) was given in an antecubital vein using a power injector (Stellant D; Medrad, Warrendale, PA, USA) at a flow rate of 4 mL/s and followed by a 20 mL saline chaser. cCTA images were analyzed on a multi-modality 3D-enabled workstation (Syngo VE36A; Siemens Healthineers, Forchheim, Germany) and interpreted by an experienced cardiovascular radiologist blinded to patient characteristics [36]. Coronary calcium was assessed with a dedicated software application according to the Agatston scoring convention (CaScore, Siemens Healthineers) [37]. Coronary artery stenosis was quantitatively graded using on-site prototype software (Coronary Plaque Analysis 2.0. syngo.via FRONTIER, Siemens Healthineers) and visually graded in accordance with SCCT guidelines as normal (< 25%), mild (25–49%), moderate (50–69%), severe (70–99%), or totally occluded. Obstructive CAD was defined as ≥ 50% luminal stenosis on cCTA [38].

Analysis of computed tomographic-based fractional flow reserve (CT-FFR$_{ML}$)

The cCTA datasets were analyzed by an on-site CT-FFR$_{ML}$ prototype software based on a machine-learning algorithm (Siemens cFFR, version 3.1; Siemens Healthineers, currently not commercially available) installed on a regular workstation (Syngo VE36A; Siemens Healthineers). For each vessel, the software semi-automatically generated vascular-specific centerlines that defined the lumen and marked the stenosis. An experienced cardiovascular radiologist who was blinded to patient clinical data reviewed the vessel boundaries and centerlines before accepting the results. The location of iFR®-measurement reviewed and then matched to cCTA by the blinded cardiovascular radiologist. Through patient specific physiological conditions (blood pressure, heart rate, left ventricular mass) and flow dynamic models a hybrid approach of the prototype software permitted the simulation of blood flow and showed the hyperaemic state in the coronary vessels [8]. Thus, a patient-specific anatomic color-coded 3-dimensional mesh of the epicardial coronary artery tree and aortic root was created. CT-FFR$_{ML}$ values could be directly evaluated by placing a marker in the vessel of interest. To validate the reproducibility of the CT-FFR$_{ML}$

results, another experienced cardiovascular radiologist, who was also blinded to patient clinical data, analyzed the same cCTA datasets with the on-site CT-FFR_{ML} prototype software. This allowed to evaluated the inter-observer variability. For the diagnosis of a hemodynamically relevant stenosis, CT-FFR_{ML} values of ≤0.80 were established as a cut-off value [22].

ICA measurement with instantaneous wave free ratio (iFR®)

An experienced senior interventional cardiologist performed the ICA as indicated under the current ESC guidelines [34]. The coronary arteries were visually evaluated and analyzed by quantitative coronary angiography software (QCA Caas Workstation, PIE Medical Imaging, Maastricht, The Netherlands). Every visually suspicious stenosis (intermediate grade 40–80%) was interrogated by iFR® intraprocedurally for hemodynamic significance according to the current ESC guidelines [34]. For this purpose, an iFR® pressure wire (Verrata™ pressure wire, Volcano Corporation, Koninklijke Philips N.V. Amsterdam, The Netherlands) was placed distally to the suspicious stenosis and iFR®-measurements were obtained during five consecutive heartbeats and was calculated with the assistance of computer software (Volcano Corporation). The optimal wave-free period for the iFR®-measurement, which is defined as a fixed period of diastole where the microvascular resistance is minimized and constant, was found intraprocedurally by the pressure curve [39]. To determine a hemodynamically significant stenosis an iFR® cut-off value ≤0.89 was chosen and is in accordance with current ESC guidelines [34].

Statistical analysis

All analyses were performed using SAS (Version 9.4 SAS Institute Inc., Cary, NC, USA). Categorical variables are presented as percentages; whereas, continuous variables are presented as either mean ± standard deviation (SD) or median with interquartile range (IQR) and were analyzed with the independent sample *t* test. Pearson statistics and an interclass correlation coefficient were applied to analyze the degree of correlation between CT-FFR_{ML} and iFR®. Moreover, a Bland–Altman analysis was performed comparing CT-FFR_{ML} and invasive iFR®-measurement on a per-lesion level. Sensitivity, specificity, positive predictive value and negative predictive value were evaluated on a per-lesion and per-patient level for cCTA (> 50%), cCTA (> 70%) and CT-FFR_{ML} (≤0.80) using iFR® (≤0.89) as the reference standard to detect lesion-specific ischemia. The area under the receiver operating characteristics curve (AUC) was determined, compared and tested by the DeLong test for cCTA, CT-FFR_{ML} and iFR® as a metric of overall diagnostic performance [40]. A *p* value of ≤0.05 was considered statistically significant.

Results

Between July 2017 and December 2018, we included 80 patients with a clinical indication for cCTA (Fig. 1). Baseline characteristics of included patients are presented in Table 1. Our study population had the following proportions of cardiovascular risk factors: 75% hypertension, 48% hyperlipidemia, 28% had a family history of CAD, 20% diabetes mellitus, and 20% were current smokers. We

Table 1 Baseline characteristics ($n = 40$)

Parameter	Mean value ± standard deviation or frequency (%)
Age (years)	67 ± 12
Men (%)	29 (73%)
Height (cm)	172 ± 9
Weight (kg)	86 ± 15
Body-mass-index (kg/m^2)	29 ± 5
Pretest probability[a] (%)	57
Prior percutaneous coronary intervention	7 (18%)
Atrial fibrillation	8 (20%)
Systolic blood pressure (mmHg)	131 ± 19
Diastolic blood pressure (mmHg)	70 ± 13
Heart rate (beats per min)	69 ± 12
Cardiovascular risk factors	
Hypertension[a]	30 (75%)
Hyperlipidemia[b]	19 (48%)
Family history of CAD	11 (28%)
Diabetes mellitus	8 (20%)
Current smoking	8 (20%)
Medication	
Angiotensin converting enzyme inhibitor or AT_1 receptor antagonists (%)	23 (58%)
B-blocker (%)	18 (45%)
Statin (%)	17 (43%)
Aspirin (%)	15 (38%)
Calcium channel blocker (%)	12 (30%)

Unless otherwise specified, data are numbers of patients with percentages in parentheses. Data are mean ± standard deviation (SD) or frequency

CAD coronary artery disease

[a]Pretest probability calculated with the CAD consortium clinical score [35]

[b]Defined as blood pressure > 140 mmHg systolic, > 90 mmHg diastolic, or use of an antihypertensive medication

[c]Defined as a total cholesterol level of > 200 mg/dL or use of antilipidemic medication

calculated a mean pretest-probability for CAD of 57% (CAD consortium clinical score) for our patient population. In 35% of the indicated cCTA cases, no relevant coronary artery stenosis could be detected. According to the current ESC guidelines an ICA is indicated when cCTA shows stenosis with luminal narrowing (30–90%) or uncertain findings are observed. This was the case in 50 patients (63%). In 84% ($n=42$), the iFR®-measurement was performed within one month to assess the hemodynamics of the suspected lesion. The iFR®-measurement was not indicated in eight patients because six cases had high-grade stenosis (> 80%) and two cases had non-obstructive stenosis that could be determined by invasive visual assessment alone. Finally, the stenosis measured by iFR® were evaluated by the on-site CT-FFR_{ML} algorithm. We were able to calculate CT-FFR_{ML} values in 40 out of 42 patients (95%). In one case, inadequate CT image quality prevented successful analysis, and in the other case the patient had prior stent placement. Example cases are presented in Figs. 2 and 3.

Within the remaining 40 patients, 57 vessel specific lesions were analyzed and 15 (26%) lesions were determined as hemodynamically relevant by iFR® ≤ 0.89. cCTA (> 50%) overestimated the severity of stenosis in 21 of 57 lesions and cCTA (> 70%) overestimated severity in 6 of 57 lesions. However, CT-FFR_{ML} revealed the absence of lesion specific ischemia, thus ruling out obstructive CAD, in 40 of 57 stenoses, which could have resulted in a substantial reduction of unnecessary ICAs on non-obstructive lesions. The mean

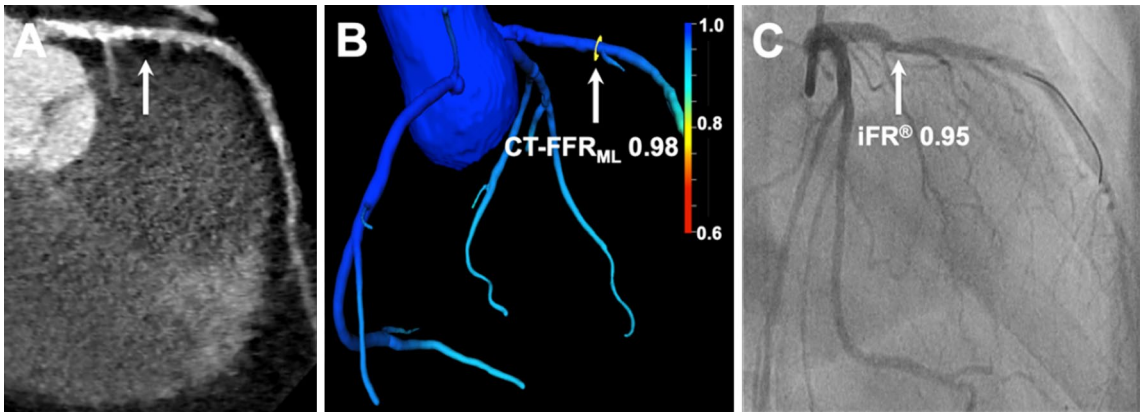

Fig. 2 58-year-old woman with history of atypical chest pain, increased cardiovascular risk profile and pre-test probability for CAD of 20%. **a** cCTA demonstrates severe stenosis (>70%) of the proximal left anterior descending coronary artery caused by calcified plaques (arrow). **b** CT-FFR_{ML} derivation, displayed in a color-coded 3-dimensional mesh, resulted in a value of 0.98 (arrow). **c** Coronary catheter angiography shows a stenosis (arrow) with an iFR® measurement of 0.95. *cCTA* coronary CT angiography, *CT-FFR_{ML}* fractional flow reserve derived from coronary computed tomography angiography based on machine learning algorithm, *iFR®* instantaneous wave free ratio

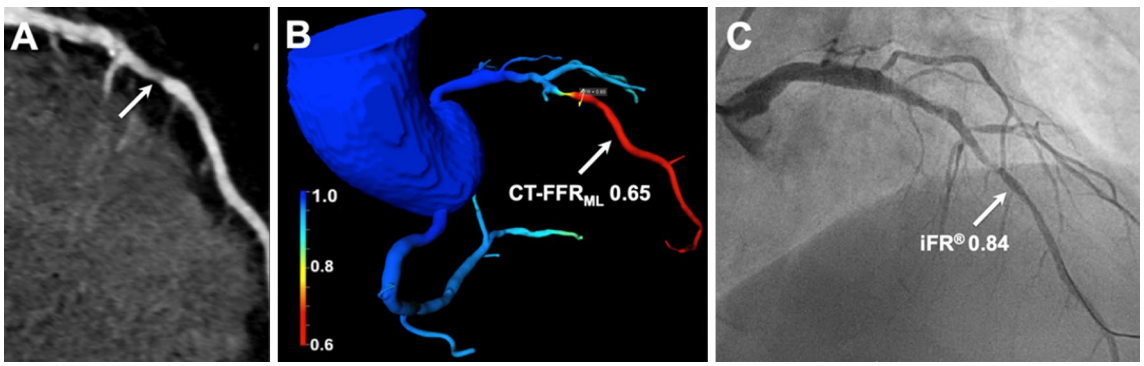

Fig. 3 67-year-old man with suspected CAD and an increased cardiovascular risk profile. **a** cCTA shows a severe, high risk stenosis (>70%) of the mid left anterior descending artery (arrow). **b** In a 3-dimensional—color-coded mesh a calculated CT-FFR_{ML} value of 0.65 is presented (arrow). **c** This high-risk stenosis (arrow) is visualized in ICA and measurement with iFR® (iFR®-value 0.84; iFR® cut-off value ≤ 0.89). Revascularization with PCI and implantation of two drug eluting stents was performed. *cCTA* coronary CT angiography, *CT-FFR_{ML}* fractional flow reserve derived from coronary computed tomography angiography based on machine learning algorithm, *iFR®* instantaneous wave free ratio, *PCI* percutaneous coronary intervention

Table 2 Findings of cCTA, CT-FFR$_{ML}$ and ICA

Parameter	Mean value ± standard deviation or frequency (%)
Coronary computed tomography	
Agatston score[a]	928 ± 981
Range[a]	0–3608
No. of patients > 400	21 (64%)
Luminal stenosis > 50%	57 (100%)
Luminal stenosis > 70%	24 (42%)
CT-FFR$_{ML}$ ≤ 0.80	15 (26%)
CT-FFR$_{ML}$ procedure time (min)	11 ± 2
Invasive coronary catheter angiography	
Left anterior descending coronary artery	31 (54%)
Left circumflex coronary artery	14 (25%)
Right coronary artery	12 (21%)
iFR® ≤ 0.89	15 (26%)

Unless otherwise specified, data are numbers of patient, with percentages in parentheses. Data are mean ± standard deviation (SD) or frequency

CT-FFR$_{ML}$ fractional flow reserve derived from coronary computed tomography angiography based on machine learning algorithm, *iFR®* instantaneous wave free ratio

[a]Agatston score was obtained in 33 patients

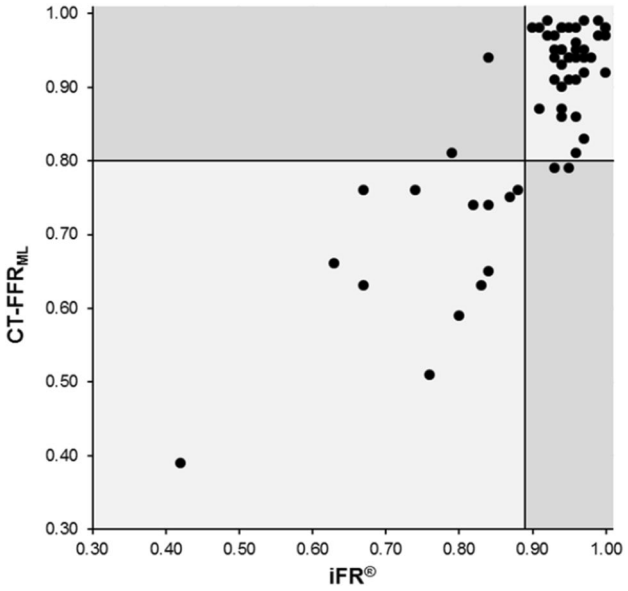

Fig. 4 Performance for determining the hemodynamic relevance of coronary artery stenosis on a per lesion basis illustrates a strong correlation between on-site CT-FFR$_{ML}$ with invasive iFR® as the reference standard (Pearson correlation coefficient $p = 0.82$, $p < 0.0001$, 95% CI 0.715–0.920). *CT-FFR$_{ML}$* fractional flow reserve derived from coronary computed tomography angiography based on machine learning algorithm, *iFR®* instantaneous wave free ratio

calculation time for CT-FFR$_{ML}$ was 11 ± 2 min. Relevant results of standard cCTA acquisition and CT-FFR$_{ML}$ analysis compared to iFR® are illustrated in Table 2. On per lesion evaluation, the correlation was $r = 0.82$ ($p < 0.0001$; 95% CI 0.715–0.920; Pearson's product-moment) (Fig. 4) with an intraclass correlation coefficient of $r = 0.76$ ($p < 0.0001$; 95% CI 0.595–0.866) between the on-site CT-FFR$_{ML}$ and iFR®. The inter-observer correlation was $r = 0.91$ ($p < 0.0001$, 95% CI 0.87–0.95). As illustrated in Fig. 5, a Bland–Altman analysis was performed and the mean differences for on-site CT-FFR$_{ML}$ and iFR® on a per lesion level was calculated at 0.078 (95% limits of agreement − 0.19 to 0.12). CT-FFR$_{ML}$ for a per-patient and per-lesion basis revealed a sensitivity of 92% (95% CI 64–99%) and 87% (95% CI 59–98%), a specificity of 96% (95% CI 81–99%) and 95% (95% CI 84–99%), a positive predictive value of 92% (95% CI 64–99%) and 87% (95% CI 59–98%), and a negative predictive value of 96% (95% CI 81–99%) and 95% (95% CI 84–99%), respectively (Table 3). In comparison, the sensitivity, specificity, positive predict value, negative predict value and accuracy for cCTA (> 50%), cCTA (> 70%) and ICA (> 50%) are also presented in Table 3, using iFR® as the reference standard. The diagnostic accuracy for the detection of hemodynamically relevant stenosis of cCTA (> 50%), cCTA (> 70%), ICA (> 50%), and CT-FFR$_{ML}$ when compared to iFR® on a per-lesion and a per-patient level was calculated to be 61% (95% CI 48–74%) and 55% (95% CI 39–71%), 81% (95% CI 68–90%) and 72% (95% CI 56–85%), 68% (95% CI 55–80%) and 70% (95% CI 54–83%), and 93% (95% CI 83–98%) and 95% (95% CI 83–99%), respectively. Notably, there was a significant improvement in the specificity between cCTA (> 50%) and CT-FFR$_{ML}$, which increased from 50% (95% CI 34–66%) to 95% (95% CI 84–99%) on a per-lesion basis and from 37% (95% CI 19–58%) to 96% (95% CI 81–99%)

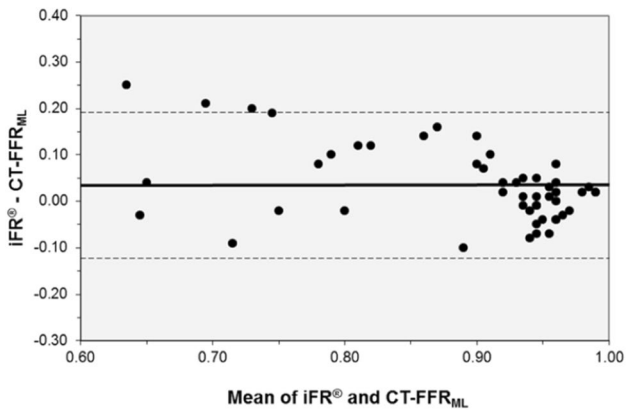

Fig. 5 Bland Altman analysis plot comparing iFR® with CT-FFR$_{ML}$ on a per lesion level. Mean difference between both techniques was 0.078 (limits of agreement − 0.19 to 0.12). *CT-FFR$_{ML}$* fractional flow reserve derived from coronary computed tomography angiography based on machine learning algorithm, *iFR®* instantaneous wave free ratio

Table 3 Diagnostic performance of fractional flow reserve from coronary computed tomography angiography, invasive coronary angiography and standard evaluation of coronary computed tomography angiography on a per-lesion and per-patient level using iFR® as the reference standard

	cCTA (>50%)	cCTA (>70%)	ICA (>50%)	CT-FFR$_{ML}$ (≤0.80)
Per-lesion ($n=57$)				
Sensitivity (%)	93 (68–99)	67 (38–88)	73 (45–92)	87 (59–98)
Specificity (%)	50 (34–66)	86 (72–95)	67 (51–80)	95 (84–99)
PPV (%)	40 (24–58)	62 (35–85)	44 (24–65)	87 (59–98)
NPV (%)	96 (77–99)	88 (74–96)	87 (71–97)	95 (84–99)
Accuracy (%)	61 (48–74)	81 (68–90)	68 (55–80)	93 (83–98)
Per-patient ($n=40$)				
Sensitivity (%)	92 (64–99)	61 (32–86)	85 (55–98)	92 (64–99)
Specificity (%)	37 (19–58)	78 (58–91)	63 (42–81)	96 (81–99)
PPV (%)	41 (23–60)	57 (29–82)	52 (30–74)	92 (64–99)
NPV (%)	91 (59–99)	81 (61–93)	90 (67–99)	96 (81–99)
Accuracy (%)	55 (39–71)	72 (56–85)	70 (54–83)	95 (83–99.)

cCTA coronary computed tomography angiography, *CT-FFR$_{ML}$* fractional flow reserve derived from coronary computed tomography angiography based on machine learning algorithm, *ICA* invasive coronary angiography, *iFR®* instantaneous wave free ratio, *NPV* negative predictive value, *PPV* positive predictive value

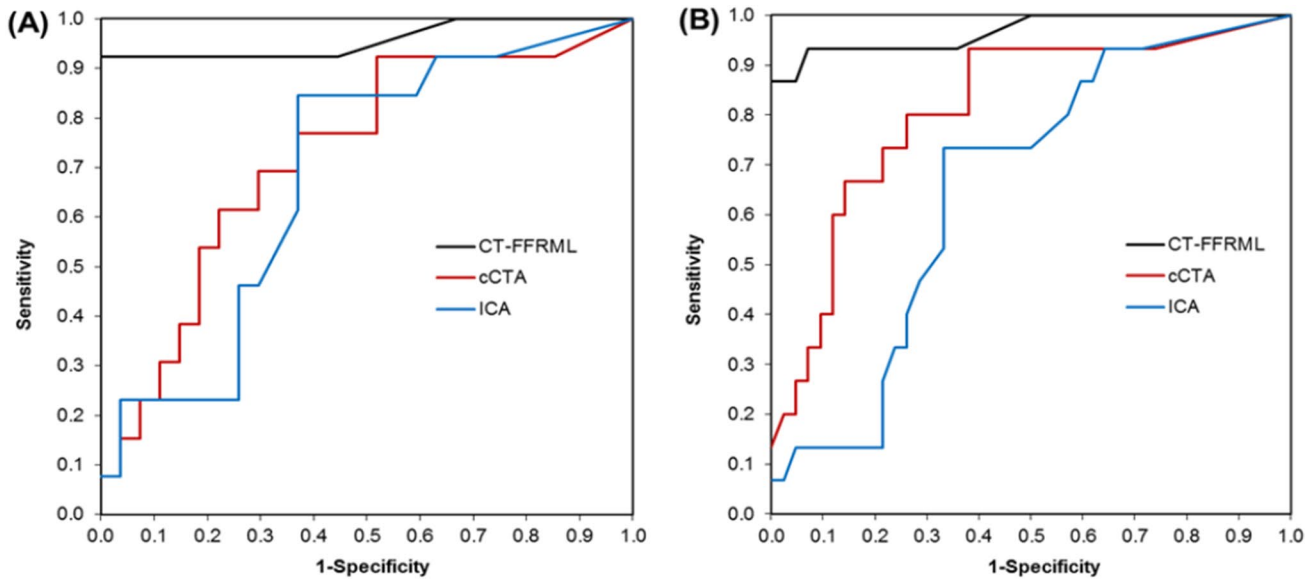

Fig. 6 On per-patient (**a**) and per-lesion level (**b**), the area under the curve for the detection of hemodynamically relevant stenosis by CT-FFR$_{ML}$ using iFR® as the reference standard were 0.96 (95% CI 0.87–1.00) and 0.97 (95% CI 0.91–1.00), respectively. By cCTA and ICA, AUC results were on, per-patient and per-lesion level, 0.72 (95% CI 0.55–0.90) and 0.81 (95% CI 0.68–0.94), and 0.68 (95% CI 0.51–0.86) and 0.66 (95% CI 0.50–0.81). *AUC* area under the curve, *cCTA* coronary CT angiography, *CT-FFR$_{ML}$* fractional flow reserve derived from coronary computed tomography angiography based on machine learning algorithm, *ICA* invasive coronary angiography, *iFR®* instantaneous wave free ratio

on a per-patient level. The area under the curve (AUC) that is illustrated in Fig. 6 shows a substantial improvement in diagnostic performance for the detection of lesion-specific ischemia with CT-FFR$_{ML}$ when compared with the mere morphological assessment by cCTA. The AUC comparison to determine lesion-specific ischemia (iFR® ≤ 0.89) reached statistical significance in the per-patient analysis ($p=0.0086$) and in the per-lesion analysis ($p=0.0196$) between cCTA and CT-FFR$_{ML}$.

Discussion

In this study, we examined an on-site CT-FFR$_{ML}$ machine learning algorithm in terms of clinical practicality and diagnostic accuracy for the determination of the hemodynamic severity of suspicious coronary lesions when compared to the current invasive reference standard of iFR®.

Our observations suggest that the CT-FFR_{ML} algorithm performs well in clinical settings. In addition, we demonstrate that the use of the on-site CT-FFR_{ML} algorithm achieves a reduction in the time needed for calculating this index. Our mean calculation time was 11 ± 2 min. Published in 2014, Renker et al. introduced an on-site computational fluid-dynamics based CT-FFR algorithm with a processing and calculation time of 37.5 ± 13.8 min [41]. Off-site CT-FFR algorithms are more time consuming in comparison; yet, the off-site FFR-CT analysis by HeartFlow Inc. (Redwood City, CA, USA) remains the only commercially and clinically available solution to date. This algorithm has attained approval by the Food and Drug Administration in 2015 and sees increasing coverage by healthcare payors, thus indicating the growing recognition of the usefulness and effectiveness of CT-FFR. Accordingly, CT-FFR is an increasingly established tool in the evolving field of coronary physiology. Various large trials such as DISCOVER-FLOW, DeFACTO, and NXT have investigated CT-FFR in comparison to invasive FFR as the reference standard for the detection of hemodynamically relevant stenosis [20–22]. The insights of these studies demonstrated that the CT-FFR strategy was significantly superior compared to the sole cCTA strategy for the determination of the hemodynamic relevance of coronary artery stenosis [20–22].

We compared the on-site CT-FFR_{ML} algorithm with a novel innovative invasive resting index without administration of adenosine. Instantaneous wave free ratio (iFR®) has gained importance for the invasive detection of hemodynamically significant coronary stenosis. This adenosine-independent approach has many advantages over the invasive FFR method and has already proven its usefulness in various studies [30, 31, 33, 39, 42]. iFR®, as a resting index, finds consideration in the guideline of the ESC on myocardial revascularization and is now of equal standing with FFR as a class IA recommendation [34]. With the use of iFR® as the reference standard, the diagnostic performance of CT-FFR_{ML} on a per-patient and per-lesion level showed high specificity [96% (95% CI 81–99%) and 95% (95% CI 84–99%)] for CT-FFR_{ML} to detect hemodynamically relevant stenosis. Our results are comparable with previous studies that have evaluated an on-site CT-FFR_{ML} approach in terms of diagnostic accuracy when compared to invasive FFR [24, 41]. Similar to previous work we observed a substantial increase in the area under the curve on a per-lesion and per patient level [AUC, 0.96 (95% CI 0.87–1.00) and 0.97 (95% CI 0.91–1.00)] to detect hemodynamically significant coronary stenosis compared to the evaluation of cCTA studies alone [20, 22, 41].

The correlation between iFR® and CT-FFR has been investigated before. In 2018, Fujimoto et al. for the first time reported a correlation coefficient of $r = 0.62$ between CT-FFR and iFR® [43]. However, in our investigation the correlation coefficient between CT-FFR_{ML} and iFR® was substantially higher with $r = 0.82$ ($p < 0.0001$; Pearson's product-moment), which is much more comparable with the results of previous investigations that had used invasive FFR as the reference standard [22, 41].

As expected, cCTA overestimated stenosis in 17/40 of our patients, which could have potentially led to a reduction in ICAs without the need of coronary intervention. In contrast to the evaluation of cCTA alone, the addition of CT-FFR_{ML} resulted in the true negative reclassification of 40 stenoses and 26 patients as free of lesion specific ischemia, which could have led to a drastic reduction in unnecessary ICAs. In contrast, CT-FFR_{ML} correctly identified 13 stenoses and 12 patients as true positive for obstructive CAD. Thus, our results are very much in line with the 2014 PLATFORM trial, which differed from the concept of other former validation studies and was able to prove a significant reduction in originally planned ICAs with utilization of CT-FFR [19]. Hlatky et al. performed a sub-analysis of the PLATFORM data and found a significant cost reduction without any adverse outcomes and enhanced quality of life [44].

Limitations

Our results are to be evaluated and considered in light of the following limitations: First, it should be noted that our study cohort of a total number of 40 enrolled patients with 57 lesions is relatively small. Second, patients had to be excluded because of prior CABG, prior stent placement, or complex bifurcation stenosis type D. These first two limitations are due to the structure of our investigation as we aimed to perform a longitudinal study over a defined period of time in a real-life clinical setting with the consideration of current ESC guidelines. Third, in our study we did not perform any comparisons to conventional invasive FFR. From a scientific point of view, comparison with FFR would have been interesting. Nevertheless, this was clinically not indicated because iFR® is now of equal standing with FFR as a class IA recommendation. Finally, we have not performed any patient follow-up for outcome determination. Rather, our primary aim was the comparison of CT-FFR_{ML} and iFR® in terms of diagnostic accuracy and testing its applicability in everyday clinical practice. Further studies will be necessary to validate our findings of CT-FFR_{ML} compared with iFR® and to provide more representative results.

Conclusions

The results of our study suggest that on-site CT-FFR_{ML} performs well in routine clinical practice. In addition, we were able to demonstrate high diagnostic accuracy of CT-FFR_{ML}

compared to iFR® as a resting index; moreover, we showed a strong correlation between CT-FFR_{ML} values and iFR® values in the detection hemodynamically significant stenosis. Further studies will be necessary to validate our findings of CT-FFR_{ML} compared with iFR® and to provide more representative results.

Acknowledgement Supported by Siemens Healthineers for providing CT-FFR_{ML} software for research purposes, which is currently not commercially available. Furthermore, the authors would like to thank Philips Volcano Corporation (Koninklijke Philips N.V. Amsterdam, The Netherland) for their support.

Funding UJS receives institutional research support and/or honoraria for consulting and speaking from Astellas, Bayer, Bracco, Elucid Bio-Imaging, GE, Guerbet, HeartFlow, and Siemens. SB receives research support from Philips Volcano. All other authors declare that they have no financial disclosures. The presented CT-FFR_{ML} software is provided by Siemens and is currently not commercially available.

References

1. Erthal F, Premaratne M, Yam Y, Chen L, Lamba J, Keenan M et al (2018) Appropriate use criteria for cardiac computed tomography: does computed tomography have incremental value in all appropriate use criteria categories? J Thorac Imaging 33(2):132–137
2. Maroules CD, Rajiah P, Bhasin M, Abbara S (2019) Current evidence in cardiothoracic imaging: growing evidence for coronary computed tomography angiography as a first-line test in stable chest pain. J Thorac Imaging 34(1):4–11
3. Patel MR, Peterson ED, Dai D, Brennan JM, Redberg RF, Anderson HV et al (2010) Low diagnostic yield of elective coronary angiography. N Engl J Med 362(10):886–895
4. Patel MR, Dai D, Hernandez AF, Douglas PS, Messenger J, Garratt KN et al (2014) Prevalence and predictors of non-obstructive coronary artery disease identified with coronary angiography in contemporary clinical practice. Am Heart J 167(6):846–852 **(e2)**
5. Meijboom WB, Meijs MF, Schuijf JD, Cramer MJ, Mollet NR, van Mieghem CA et al (2008) Diagnostic accuracy of 64-slice computed tomography coronary angiography: a prospective, multicenter, multivendor study. J Am Coll Cardiol 52(25):2135–2144
6. The SC (2015) CT coronary angiography in patients with suspected angina due to coronary heart disease (SCOT-HEART): an open-label, parallel-group, multicentre trial. Lancet (London, England) 385(9985):2383–2391
7. Bittner DO, Ferencik M, Douglas PS, Hoffmann U (2016) Coronary CT angiography as a diagnostic and prognostic tool: perspective from a multicenter randomized controlled trial: PROMISE. Curr Cardiol Rep 18(5):40
8. Taylor CA, Fonte TA, Min JK (2013) Computational fluid dynamics applied to cardiac computed tomography for non-invasive quantification of fractional flow reserve: scientific basis. J Am Coll Cardiol 61(22):2233–2241
9. Renker M, Schoepf UJ, Becher T, Krampulz N, Kim W, Rolf A et al (2017) Computed tomography in patients with chronic stable angina: fractional flow reserve measurement. Herz 42(1):51–57
10. Wang R, Renker M, Schoepf UJ, Wichmann JL, Fuller SR, Rier JD et al (2015) Diagnostic value of quantitative stenosis predictors with coronary CT angiography compared to invasive fractional flow reserve. Eur J Radiol 84(8):1509–1515
11. Baumann S, Becher T, Schoepf UJ, Lossnitzer D, Henzler T, Akin I et al (2017) Fractional flow reserve derived by coronary computed tomography angiography: a sophisticated analysis method for detecting hemodynamically significant coronary stenosis. Herz 42(6):604–606
12. Schmermund A, Eckert J, Schmidt M, Magedanz A, Voigtlander T (2018) Coronary computed tomography angiography: a method coming of age. Clin Res Cardiol 107(Suppl 2):40–48
13. Ihdayhid AR, Sakaguchi T, Linde JJ, Sorgaard MH, Kofoed KF, Fujisawa Y et al (2018) Performance of computed tomography-derived fractional flow reserve using reduced-order modelling and static computed tomography stress myocardial perfusion imaging for detection of haemodynamically significant coronary stenosis. Eur Heart J Cardiovasc Imaging 19(11):1234–1243
14. Schuijf JD, Ko BS, Di Carli MF, Hislop-Jambrich J, Ihdayhid AR, Seneviratne SK et al (2018) Fractional flow reserve and myocardial perfusion by computed tomography: a guide to clinical application. Eur Heart J Cardiovasc Imaging 19(2):127–135
15. Schwartz FR, Koweek LM, Norgaard BL (2019) Current evidence in cardiothoracic imaging: computed tomography-derived fractional flow reserve in stable chest pain. J Thorac Imaging 34(1):12–17
16. Benton SM Jr, Tesche C, De Cecco CN, Duguay TM, Schoepf UJ, Bayer RR 2nd (2018) Noninvasive derivation of fractional flow reserve from coronary computed tomographic angiography: a review. J Thorac Imaging 33(2):88–96
17. Baumann S, Akin I, Borggrefe M, Ball BD Jr, Schoepf UJ, Renker M (2016) Different approaches for coronary computed tomography angiography-derived versus invasive fractional flow reserve assessment. Am J Cardiol 117(3):486
18. Gonzalez JA, Lipinski MJ, Flors L, Shaw PW, Kramer CM, Salerno M (2015) Meta-analysis of diagnostic performance of coronary computed tomography angiography, computed tomography perfusion, and computed tomography-fractional flow reserve in functional myocardial ischemia assessment versus invasive fractional flow reserve. Am J Cardiol 116(9):1469–1478
19. Douglas PS, Pontone G, Hlatky MA, Patel MR, Norgaard BL, Byrne RA et al (2015) Clinical outcomes of fractional flow reserve by computed tomographic angiography-guided diagnostic strategies vs. usual care in patients with suspected coronary artery disease: the prospective longitudinal trial of FFR (CT): outcome and resource impacts study. Eur Heart J 36(47):3359–3367
20. Koo BK, Erglis A, Doh JH, Daniels DV, Jegere S, Kim HS et al (2011) Diagnosis of ischemia-causing coronary stenoses by noninvasive fractional flow reserve computed from coronary computed tomographic angiograms. Results from the prospective multicenter DISCOVER-FLOW (Diagnosis of Ischemia-Causing Stenoses Obtained Via Noninvasive Fractional Flow Reserve) study. J Am Coll Cardiol 58(19):1989–1997
21. Min JK, Leipsic J, Pencina MJ, Berman DS, Koo BK, van Mieghem C et al (2012) Diagnostic accuracy of fractional flow reserve from anatomic CT angiography. JAMA 308(12):1237–1245
22. Norgaard BL, Leipsic J, Gaur S, Seneviratne S, Ko BS, Ito H et al (2014) Diagnostic performance of noninvasive fractional flow reserve derived from coronary computed tomography angiography in suspected coronary artery disease: the NXT trial (Analysis of Coronary Blood Flow Using CT Angiography: Next Steps). J Am Coll Cardiol 63(12):1145–1155
23. Coenen A, Kim YH, Kruk M, Tesche C, De Geer J, Kurata A et al (2018) Diagnostic accuracy of a machine-learning approach to coronary computed tomographic angiography-based fractional flow reserve: result from the MACHINE consortium. Circ Cardiovasc Imaging 11(6):e007217
24. Tesche C, De Cecco CN, Baumann S, Renker M, McLaurin TW, Duguay TM et al (2018) Coronary CT angiography-derived fractional flow reserve: machine learning algorithm versus computational fluid dynamics modeling. Radiology 288(1):64–72

25. Windecker S, Kolh P, Alfonso F, Collet JP, Cremer J, Falk V et al (2014) 2014 ESC/EACTS guidelines on myocardial revascularization: the task force on myocardial revascularization of the European Society of Cardiology (ESC) and the European Association for Cardio-Thoracic Surgery (EACTS)Developed with the special contribution of the European Association of Percutaneous Cardiovascular Interventions (EAPCI). Eur Heart J 35(37):2541–2619
26. Wolk MJ, Bailey SR, Doherty JU, Douglas PS, Hendel RC, Kramer CM et al (2014) ACCF/AHA/ASE/ASNC/HFSA/HRS/SCAI/SCCT/SCMR/STS 2013 multimodality appropriate use criteria for the detection and risk assessment of stable ischemic heart disease: a report of the American College of Cardiology Foundation Appropriate Use Criteria Task Force, American Heart Association, American Society of Echocardiography, American Society of Nuclear Cardiology, Heart Failure Society of America, Heart Rhythm Society, Society for Cardiovascular Angiography and Interventions, Society of Cardiovascular Computed Tomography, Society for Cardiovascular Magnetic Resonance, and Society of Thoracic Surgeons. J Am Coll Cardiol 63(4):380–406
27. Harle T, Meyer S, Vahldiek F, Elsasser A (2016) Differences between automatically detected and steady-state fractional flow reserve. Clin Res Cardiol 105(2):127–134
28. Harle T, Zeymer U, Hochadel M, Zahn R, Kerber S, Zrenner B et al (2017) Real-world use of fractional flow reserve in Germany: results of the prospective ALKK coronary angiography and PCI registry. Clin Res Cardiol 106(2):140–150
29. Kleiman NS (2011) Bringing it all together: integration of physiology with anatomy during cardiac catheterization. J Am Coll Cardiol 58(12):1219–1221
30. Gotberg M, Christiansen EH, Gudmundsdottir IJ, Sandhall L, Danielewicz M, Jakobsen L et al (2017) Instantaneous wave-free ratio versus fractional flow reserve to guide PCI. N Engl J Med 376(19):1813–1823
31. Davies JE, Sen S, Dehbi HM, Al-Lamee R, Petraco R, Nijjer SS et al (2017) Use of the instantaneous wave-free ratio or fractional flow reserve in PCI. N Engl J Med 376(19):1824–1834
32. Sen S, Escaned J, Malik IS, Mikhail GW, Foale RA, Mila R et al (2012) Development and validation of a new adenosine-independent index of stenosis severity from coronary wave-intensity analysis: results of the ADVISE (ADenosine Vasodilator Independent Stenosis Evaluation) study. J Am Coll Cardiol 59(15):1392–1402
33. Harle T, Bojara W, Meyer S, Elsasser A (2015) Comparison of instantaneous wave-free ratio (iFR) and fractional flow reserve (FFR)—first real world experience. Int J Cardiol 199:1–7
34. Neumann FJ, Sousa-Uva M, Ahlsson A, Alfonso F, Banning AP, Benedetto U et al (2018) 2018 ESC/EACTS guidelines on myocardial revascularization. Eur Heart J 40:87–165
35. Bittencourt MS, Hulten E, Polonsky TS, Hoffman U, Nasir K, Abbara S et al (2016) European Society of Cardiology-recommended coronary artery disease consortium pretest probability scores more accurately predict obstructive coronary disease and cardiovascular events than the diamond and forrester score: the partners registry. Circulation 134(3):201–211
36. Caselli C, De Graaf MA, Lorenzoni V, Rovai D, Marinelli M, Del Ry S et al (2015) HDL cholesterol, leptin and interleukin-6 predict high risk coronary anatomy assessed by CT angiography in patients with stable chest pain. Atherosclerosis 241(1):55–61
37. Agatston AS, Janowitz WR, Hildner FJ, Zusmer NR, Viamonte M Jr, Detrano R (1990) Quantification of coronary artery calcium using ultrafast computed tomography. J Am Coll Cardiol 15(4):827–832
38. Leipsic J, Abbara S, Achenbach S, Cury R, Earls JP, Mancini GJ et al (2014) SCCT guidelines for the interpretation and reporting of coronary CT angiography: a report of the Society of Cardiovascular Computed Tomography Guidelines Committee. J Cardiovasc Comput Tomogr 8(5):342–358
39. Escaned J, Echavarria-Pinto M, Garcia-Garcia HM, van de Hoef TP, de Vries T, Kaul P et al (2015) Prospective assessment of the diagnostic accuracy of instantaneous wave-free ratio to assess coronary stenosis relevance: results of ADVISE II International, Multicenter Study (ADenosine Vasodilator Independent Stenosis Evaluation II). JACC Cardiovasc Interv 8(6):824–833
40. DeLong ER, DeLong DM, Clarke-Pearson DL (1988) Comparing the areas under two or more correlated receiver operating characteristic curves: a nonparametric approach. Biometrics 44(3):837–845
41. Renker M, Schoepf UJ, Wang R, Meinel FG, Rier JD, Bayer RR 2nd et al (2014) Comparison of diagnostic value of a novel noninvasive coronary computed tomography angiography method versus standard coronary angiography for assessing fractional flow reserve. Am J Cardiol 114(9):1303–1308
42. Gotberg M, Cook CM, Sen S, Nijjer S, Escaned J, Davies JE (2017) The evolving future of instantaneous wave-free ratio and fractional flow reserve. J Am Coll Cardiol 70(11):1379–1402
43. Fujimoto S, Kawasaki T, Kumamaru KK, Kawaguchi Y, Dohi T, Okonogi T et al (2018) Diagnostic performance of on-site computed CT-fractional flow reserve based on fluid structure interactions: comparison with invasive fractional flow reserve and instantaneous wave-free ratio. Eur Heart J Cardiovasc Imaging 20:343–352
44. Hlatky MA, De Bruyne B, Pontone G, Patel MR, Norgaard BL, Byrne RA et al (2015) Quality-of-life and economic outcomes of assessing fractional flow reserve with computed tomography angiography: PLATFORM. J Am Coll Cardiol 66(21):2315–2323

Affiliations

Stefan Baumann[1,2,11] · Markus Hirt[1,2] · U. Joseph Schoepf[3] · Marlon Rutsch[1,2] · Christian Tesche[4] · Matthias Renker[5] · Joseph W. Golden[3] · Sebastian J. Buss[6] · Tobias Becher[1,2,7] · Waldemar Bojara[8] · Christel Weiss[9] · Theano Papavassiliu[1,2] · Ibrahim Akin[1,2] · Martin Borggrefe[1,2] · Stefan O. Schoenberg[10] · Holger Haubenreisser[10] · Daniel Overhoff[10] · Dirk Lossnitzer[1,2]

1 First Department of Medicine-Cardiology, University Medical Centre Mannheim, Mannheim, Germany

2 DZHK (German Centre for Cardiovascular Research), Partner Site Heidelberg/Mannheim, Mannheim, Germany

3 Division of Cardiovascular Imaging, Department of Radiology and Radiological Science, Medical University of South Carolina, Charleston, SC, USA

4 Department of Internal Medicine, St. Johannes-Hospital, Dortmund, Germany

5 Department of Cardiology, Kerckhoff Heart Center, Bad Nauheim, Germany

6 The Radiology Center, Sinsheim-Eberbach-Erbach-Walldorf-Heidelberg, Heidelberg, Germany

[7] Laboratory of Molecular Metabolism, The Rockefeller University, New York, NYC, USA

[8] Community Clinic Mittelrhein, Kemperhof II, The Cardiology Clinic, Koblenz, Germany

[9] Medical Faculty Mannheim, Department of Medical Statistics and Biomathematics, University Medical Center Mannheim, Heidelberg University, Mannheim, Germany

[10] University Medical Center Mannheim, Faculty of Medicine Mannheim, Institute of Clinical Radiology and Nuclear Medicine, Heidelberg University, Mannheim, Germany

[11] First Department of Medicine, Faculty of Medicine Mannheim, University Medical Centre Mannheim (UMM), University of Heidelberg, Theodor-Kutzer-Ufer 1-3, 68167 Mannheim, Germany